Article

Cell Stem Cell

Macrophage-Derived Extracellular Succinate Licenses Neural Stem Cells to Suppress Chronic Neuroinflammation

Graphical Abstract

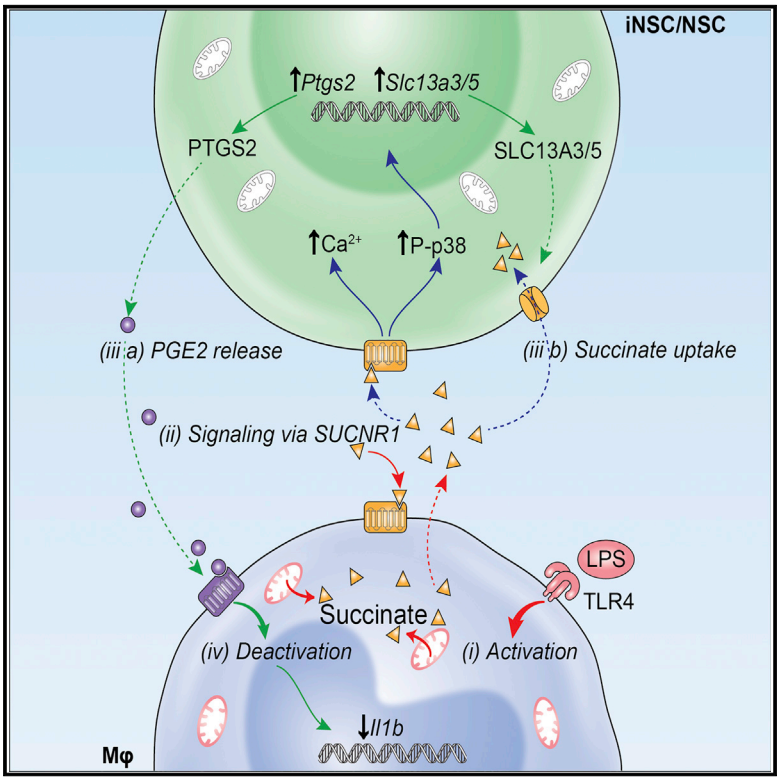

Highlights

- NSCs from somatic tissues or direct reprogramming equally repress neuroinflammation
- Extracellular succinate activates SUCNR1/GPR91 on NSCs
- Activated NSCs secrete PGE2 and scavenge succinate, thus reprogramming type 1 MPs
- *Sucnr1* mutant NSCs have reduced anti-inflammatory activity after transplantation

Authors

Luca Peruzzotti-Jametti, Joshua D. Bernstock, Nunzio Vicario, ..., Frank Edenhofer, Christian Frezza, Stefano Pluchino

Correspondence

lp429@cam.ac.uk (L.P.-J.), frank.edenhofer@uibk.ac.at (F.E.), cf366@mrc-cu.cam.ac.uk (C.F.), spp24@cam.ac.uk (S.P.)

In Brief

Peruzzotti-Jametti et al. demonstrate that somatic and directly induced brain stem cells injected into the cerebrospinal fluid of mice with experimental multiple sclerosis ameliorate chronic neuroinflammation. Grafted stem cells use SUCNR1 to decrease the inflammatory metabolite succinate, thus inducing a metabolic switch in endogenous macrophages and microglia toward an anti-inflammatory phenotype.

Peruzzotti-Jametti et al., 2018, Cell Stem Cell *22*, 1–14
March 1, 2018
https://doi.org/10.1016/j.stem.2018.01.020

CellPress

Please cite this article in press as: Peruzzotti-Jametti et al., Macrophage-Derived Extracellular Succinate Licenses Neural Stem Cells to Suppress Chronic Neuroinflammation, Cell Stem Cell (2018), https://doi.org/10.1016/j.stem.2018.01.020

Cell Stem Cell
Article

Macrophage-Derived Extracellular Succinate Licenses Neural Stem Cells to Suppress Chronic Neuroinflammation

Luca Peruzzotti-Jametti,[1,*] Joshua D. Bernstock,[1,2,8] Nunzio Vicario,[1,8] Ana S.H. Costa,[3] Chee Keong Kwok,[4] Tommaso Leonardi,[1] Lee M. Booty,[5] Iacopo Bicci,[1] Beatrice Balzarotti,[1] Giulio Volpe,[1] Giulia Mallucci,[1] Giulia Manferrari,[1] Matteo Donegà,[1] Nunzio Iraci,[1,7] Alice Braga,[1] John M. Hallenbeck,[2] Michael P. Murphy,[5] Frank Edenhofer,[4,6,*] Christian Frezza,[3,*] and Stefano Pluchino[1,9,*]

[1]Department of Clinical Neurosciences and NIHR Biomedical Research Centre, University of Cambridge, Cambridge, UK
[2]Stroke Branch, National Institute of Neurological Disorders and Stroke, NIH (NINDS/NIH), Bethesda, MD, USA
[3]MRC Cancer Unit, Hutchison/MRC Research Centre, University of Cambridge, Cambridge, UK
[4]Institute of Anatomy and Cell Biology, University of Würzburg, Würzburg, Germany
[5]MRC Mitochondrial Biology Unit, Hills Road, University of Cambridge, Cambridge, UK
[6]Institute of Molecular Biology and CMBI, Genomics, Stem Cell Biology and Regenerative Medicine, Leopold-Franzens-University Innsbruck, Innsbruck, Austria
[7]Department of Biomedical and Biotechnological Sciences (BIOMETEC), University of Catania, Via S. Sofia 97, Catania 95125, Italy
[8]These authors contributed equally
[9]Lead Contact
*Correspondence: lp429@cam.ac.uk (L.P.-J.), frank.edenhofer@uibk.ac.at (F.E.), cf366@mrc-cu.cam.ac.uk (C.F.), spp24@cam.ac.uk (S.P.)
https://doi.org/10.1016/j.stem.2018.01.020

SUMMARY

Neural stem cell (NSC) transplantation can influence immune responses and suppress inflammation in the CNS. Metabolites, such as succinate, modulate the phenotype and function of immune cells, but whether and how NSCs are also activated by such immunometabolites to control immunoreactivity and inflammatory responses is unclear. Here, we show that transplanted somatic and directly induced NSCs ameliorate chronic CNS inflammation by reducing succinate levels in the cerebrospinal fluid, thereby decreasing mononuclear phagocyte (MP) infiltration and secondary CNS damage. Inflammatory MPs release succinate, which activates succinate receptor 1 (SUCNR1)/GPR91 on NSCs, leading them to secrete prostaglandin E2 and scavenge extracellular succinate with consequential anti-inflammatory effects. Thus, our work reveals an unexpected role for the succinate-SUCNR1 axis in somatic and directly induced NSCs, which controls the response of stem cells to inflammatory metabolic signals released by type 1 MPs in the chronically inflamed brain.

INTRODUCTION

Advances in stem cell biology have raised hopes that diseases of the CNS may be ameliorated by non-hematopoietic stem cell medicines (Martino and Pluchino, 2006). We have provided compelling evidence that the transplantation of somatic neural stem cells (NSCs) improves the clinico-pathological features of animal models of inflammatory CNS disorders. Beyond the structural replacement of injured CNS cells, our work has shown that transplanted NSCs engage in complex stem cell graft-to-host communication programs, overall leading to trophic support and modulation of adaptive and innate immune responses (Bacigaluppi et al., 2009, 2016; Pluchino and Cossetti, 2013; Pluchino et al., 2005, 2009b). Specifically, NSC transplants reduce the burden of inflammation at site of injury (Pluchino et al., 2005, 2009a), decrease the number of type 1 inflammatory mononuclear phagocytes (MPs) (Cusimano et al., 2012), and promote the healing of the injured CNS via yet poorly characterized mechanisms.

However, the clinical translation of experimental NSC therapies is still limited by the sources from which human NSCs (hNSCs) are derived (Anderson et al., 2017), the intrinsic immunogenicity of allogeneic hNSC lines (Ramos-Zúñiga et al., 2012; Rice et al., 2013), and the stability of the so-called "intended clinical cell lot" (Anderson et al., 2017; Wright et al., 2006). Autologous and stably expandable directly induced NSCs (iNSCs) from patients' dermal fibroblasts are emerging as a valid alternative to NSC therapies (Lu et al., 2013; Meyer et al., 2015; Thier et al., 2012). The direct reprogramming into iNSCs avoids the laborious progression through a pluripotent state and subsequent differentiation into desired lineages described for induced pluripotent stem cell (iPSC) technology (Meyer et al., 2015; Thier et al., 2012). Therefore, making stably expandable iNSCs from somatic cells represents the most feasible way of obtaining autologous brain stem cells for downstream clinical applications (Wörsdörfer et al., 2013). However, the efficacy of directly reprogrammed iNSCs in treating inflammatory CNS disorders has not yet been tested.

In progressive forms of multiple sclerosis (MS), chronic CNS inflammation is sustained by widespread activation of MPs that include both CNS resident microglia and monocyte-derived infiltrating macrophages (Mallucci et al., 2015). MPs are found in

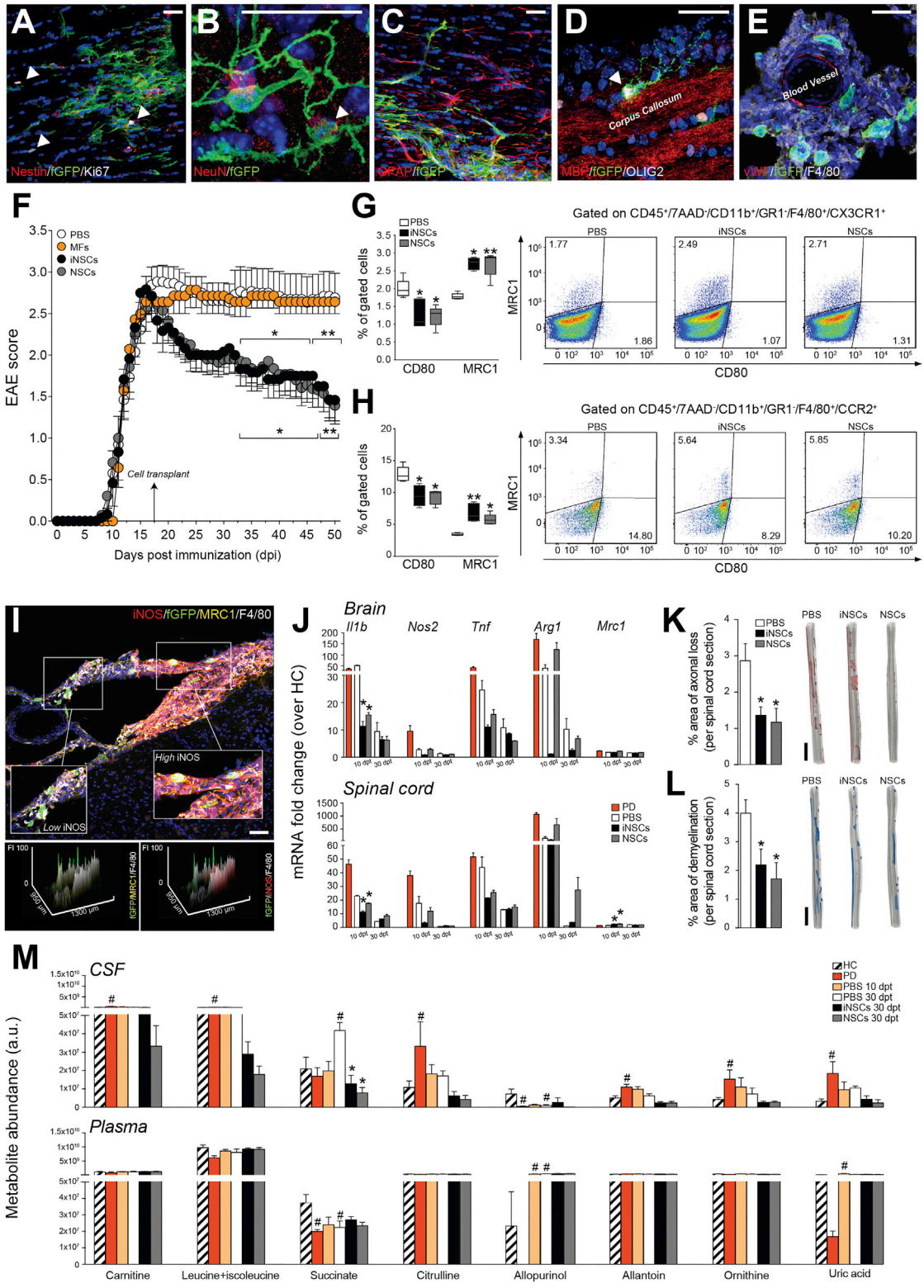

Figure 1. NSCs Transplantation Ameliorates Chronic Neuroinflammation and Reduces Succinate Levels in the CSF of EAE Mice

(A–D) Representative images of fGFP$^+$ iNSCs at 30 dpt expressing the proliferation marker Ki67 (A, arrowheads) and the neural marker Nestin (A), the mature neuronal marker NeuN (B, arrowhead), the astroglial lineage marker GFAP (C), or the oligodendroglial lineage marker OLIG2 (D, arrowhead).

(E) Confocal microscopy image of a perivascular area with several fGFP$^+$ iNSCs in juxtaposition to fGFP$^-$/F4/80$^+$ MPs. Nuclei in (A)–(E) are stained with DAPI (blue).

(legend continued on next page)

gray matter lesions, close to degenerating neurites and neuronal cell bodies (Peterson et al., 2001), and in white matter lesions, where the external rim of activated microglia is associated with chronic tissue damage (Bramow et al., 2010; Prineas et al., 2001). Areas of normal-appearing white matter are also characterized by MP accumulation, which leads to the formation of microglial nodules that drive disease pathology irrespective of concomitant T cell activation (Moll et al., 2011). The detrimental role of chronic MP-driven inflammation in progressive MS is also supported by evidence in animal disease models, where its overall burden correlates with impaired neuronal function (Planche et al., 2017), brain atrophy (Tambalo et al., 2015), and reduced regenerative responses (Jiang et al., 2014).

Activation of MPs by pro-inflammatory stimuli causes a metabolic switch toward glycolysis and reduced oxidative phosphorylation (OXPHOS) (Kelly and O'Neill, 2015). Recent evidence suggests that, within this metabolic rewiring, type 1 inflammatory MPs accumulate succinate, with important pathophysiological implications (Tannahill et al., 2013). Intracellular succinate inhibits the activity of prolyl hydroxylases enzymes (PHDs), thereby stabilizing hypoxia responsive element (HIF)-1α and inducing the transcription of interleukin (IL)-1β (Tannahill et al., 2013). Furthermore, oxidation of succinate by succinate dehydrogenase (SDH) repurposes mitochondria from ATP synthesis to reactive oxygen species (ROS) production as additional pro-inflammatory signal (Mills et al., 2016). Type 1 inflammatory MPs also release succinate extracellularly and upregulate its cognate succinate receptor 1 (SUCNR1), a G-protein-coupled receptor (also known as GPR91), which functions as autocrine and paracrine sensor to enhance IL-1β production (Littlewood-Evans et al., 2016).

As such, metabolism is emerging as an important therapeutic target to modulate the activation of both macrophages (Kelly and O'Neill, 2015) and microglia (Orihuela et al., 2016), and succinate-related pathways have key immune modulatory functions for acute and chronic inflammatory diseases (Ryu et al., 2003; Tannahill et al., 2015).

Given the established immune modulatory properties of NSCs (Pluchino and Cossetti, 2013), we hypothesized that NSCs may exert their therapeutic effects in chronic neuroinflammation by modulating MP metabolism toward reduction of secondary CNS damage.

In this work, we investigated the molecular mechanisms that underpin the capacity of somatic and directly induced NSCs to counteract the metabolic changes of type 1 inflammatory MPs both *in vivo* and *in vitro*. We show that transplanted iNSCs and NSCs are functionally equivalent in ameliorating chronic neuroinflammation in mice with experimental autoimmune encephalomyelitis (EAE). Transplanted iNSCs/NSCs switch in the activation profile of CNS-resident microglia and monocyte-derived infiltrating macrophages toward an anti-inflammatory phenotype, as well as reduce the levels of the immunometabolite succinate in the cerebrospinal fluid (CSF). iNSCs/NSCs also decrease extracellular succinate released by type 1 inflammatory MPs to reprogram their metabolism toward OXPHOS *in vitro*. Mechanistically, we show that succinate secreted by type 1 MPs elicits in iNSCs/NSCs a signaling cascade downstream SUCNR1, which enables their anti-inflammatory activity. This succinate-licensed anti-inflammatory function of iNSCs/NSCs is mediated by the secretion of prostaglandin (PG) E2, as well as by considerable scavenging of extracellular succinate. Loss of *Sucnr1* function in NSCs leads to significantly reduced anti-inflammatory activities *in vitro* and *in vivo* after transplantation in EAE.

Our study uncovers a succinate-SUCNR1 axis that clarifies how NSCs respond to inflammatory metabolic signals to inhibit the activation of type 1 MPs in chronic neuroinflammation.

RESULTS

NSC Transplantation Ameliorates Chronic Neuroinflammation and Is Coupled with Reduction of the Immunometabolite Succinate in the Cerebrospinal Fluid

We first assessed the effects of the intracerebroventricular (icv) transplantation at peak of disease (PD) of iNSCs or NSCs in mice with MOG35-55-induced chronic EAE and compared it to PBS-treated control EAE mice. Prior to transplantation, iNSCs and NSCs were expanded, characterized (Figure S1), and labeled with farnesylated (f)GFP *in vitro*. At 30 days post-transplantation (dpt), iNSC and NSC transplants survived, distributed, and integrated within the EAE brain and spinal cord (Figure S2). Only a minority of retrieved fGFP$^+$ cells (iNSCs: 2.1% ± 0.9%; NSCs: 1.7% ± 0.1%) were proliferating (Figure 1A) or expressing neuronal (Figure 1B), astroglial (Figure 1C), or oligodendroglial

(F) Behavioral outcome of iNSCs/NSCs-transplanted EAE mice. Data are mean EAE score (±SEM) from n ≥ 7 mice/group over n = 2 independent experiments. EAE mice injected icv with mouse fibroblasts (MFs) or PBS were used as controls.

(G and H) Flow-cytometry-based *ex vivo* quantification of the expression levels of type 1 inflammatory (CD80) and anti-inflammatory (MRC1) markers in CX3CR1$^+$ microglial cells (G) and CCR2$^+$ monocyte-derived infiltrating macrophages (H) from the CNS of iNSC- and NSC-transplanted EAE mice at 30 dpt. Quantitative data are shown on the left, whereas representative density plots are shown on the right. Data are min to max % of marker-positive cells from n ≥ 4 pools of mice/group.

(I) Representative confocal microscopy image and comparative histograms of a perivascular area with several fGFP$^+$ iNSCs in juxtaposition to F4/80$^+$ MPs. Low iNOS and prevalent MRC1 expression is detected in F4/80$^+$ MPs close to fGFP$^+$ iNSCs (inset on the left), whereas high iNOS expression is observed in the remaining MP infiltrate (inset on the right). Nuclei are stained with DAPI.

(J) Expression levels (qRT-PCR) of pro- and anti-inflammatory genes in the brain and spinal cord of EAE mice. Data are mean fold change over HC from n ≥ 3 mice/group.

(K and L) Quantification and representative 3D reconstructions of spinal cord damage in iNSC- and NSC-transplanted EAE mice. Data are mean % of Bielschowsky negative-stained axonal loss (K) or Luxol fast blue (LFB) negative-stained demyelinated (L) areas/spinal cord section (±SEM) from n ≥ 5 mice/group over n = 2 independent experiments.

(M) Levels of CSF metabolites significantly changed during EAE (versus HC). Corresponding levels in matched plasma samples are also shown. Data are mean a.u. (±SEM) from n ≥ 3 mice/group.

The scale bars represent 25 μm (A–E), 50 μm (I), and 2 mm (K and L). *p ≤ 0.05 and **p ≤ 0.01 versus PBS; #p ≤ 0.05 versus HC; dpt, days post-transplantation; FI, fluorescence intensity; HC, healthy controls; PD, peak of disease. See also Figures S1, S2, and S3 and Table S1.

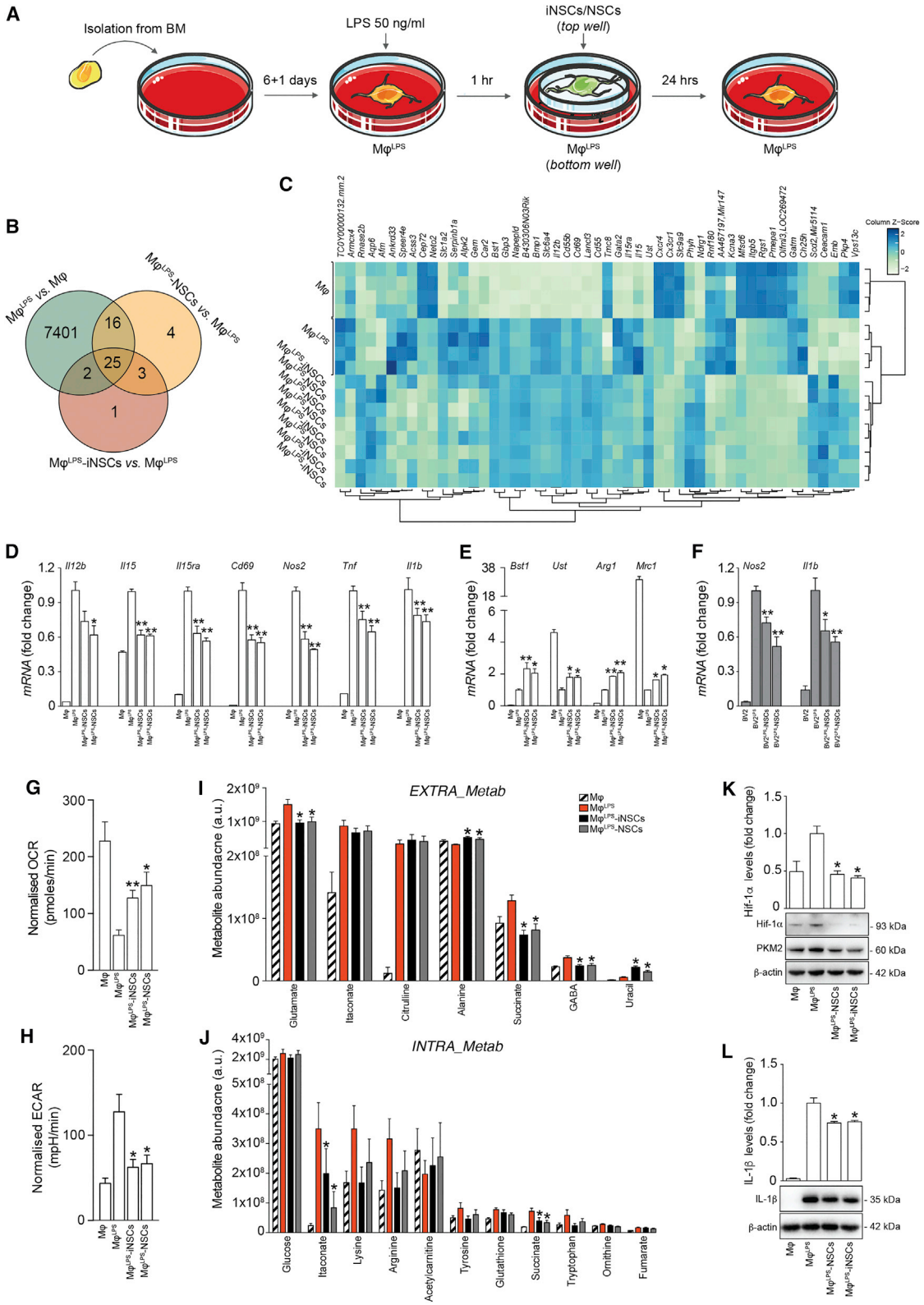

(legend on next page)

(Figure 1D) lineage markers (Figure S2). The majority (~75%) of iNSCs surviving to transplantation were found instead not to be expressing any of the neural lineage markers tested and localizing around meningeal perivascular niche-like areas close to F4/80$^+$ endogenous MPs (Figure 1E), as observed in somatic NSC grafts (Cusimano et al., 2012; Pluchino et al., 2003). The transplantation of iNSCs induced a significant and long-lasting (up to 90 dpt) amelioration of EAE scores, which started from 15 to 20 dpt onward (Figures 1F and S2). Functional recovery was also confirmed by computer-assisted automated gait analysis (Figure S2). Overall, icv-transplanted iNSCs were safe and led to behavioral and pathological recovery.

We then analyzed the composition of CNS inflammatory infiltrates via *ex vivo* flow cytometry in iNSC- and NSC-transplanted versus PBS-treated control EAE mice. The transplantation of iNSCs or NSCs had no effects on the fraction of CNS-infiltrating T cells, B cells, and total MPs, as well as in that of CD3$^+$/CD4$^+$ T cell subsets (including Th1, Th2, Treg, ThGM-CSF, and Th17 subsets) at 30 dpt (Figure S3). Instead, iNSC- or NSC-transplanted EAE mice showed a significant switch in the activation profile of CX3CR1$^+$ cells with ~1.5-fold decrease of the CD80$^+$ type 1 inflammatory microglia and parallel increase of the MRC1$^+$ anti-inflammatory microglia (Figure 1G). Likewise, CNS-infiltrating (monocyte-derived) CCR2$^+$ macrophages from iNSC- or NSC-transplanted EAE mice underwent significant phenotype switch with ~1.3-fold decrease of the CD80$^+$ type 1 inflammatory macrophages and parallel ~1.8-fold increase of the MRC1$^+$ anti-inflammatory macrophages (Figure 1H). This effect was accompanied by a significant reduction of the expression of the type 1 inflammatory MP marker inducible nitric oxide synthase (iNOS) by F4/80$^+$ MPs *in vivo* (Figures 1I and S3).

We then analyzed the expression levels of the main pro- and anti-inflammatory genes in the whole CNS. iNSC- and NSC-transplanted EAE mice both exhibited significantly reduced levels of *interleukin-1 beta* (*Il1b*) in the brain and spinal cord and increased levels of *mannose receptor C type 1* (*Mrc1*) in the spinal cord, both at 10 dpt (Figure 1J).

We found no significant differences in blood-brain barrier (BBB) permeability at 30 dpt when comparing iNSC-/NSC-transplanted with PBS-treated control EAE mice (Figure S3).

Finally, iNSC- and NSC-transplanted EAE mice accumulated significantly reduced axonal loss (Figure 1K) and demyelination (Figure 1L) in the spinal cord.

Given the established importance of metabolism in regulating the phenotype and function of MPs, we investigated whether NSC transplants affected the neuroinflammatory metabolic microenvironment. To this end, we performed an untargeted metabolic profiling of polar metabolites by liquid chromatography coupled to mass spectrometry (LC-MS) of matched CSF and plasma samples (Table S1). PBS-treated control EAE mice showed a significant increase of several CSF (but not plasma) metabolites, among which succinate only peaked at 45 days post-immunization (dpi) (corresponding to 30 dpt; Figure 1M). EAE mice not subjected to surgery also showed a significant increased succinate only in the CSF at 45 dpi (versus healthy control mice), which was not different from the levels of succinate in the CSF PBS-treated control EAE mice (Figure S3).

Whereas we did not detect any significant change in plasma metabolite levels between iNSC/NSC-transplanted and PBS-treated control EAE mice (Table S1), we found that the transplantation of iNSCs or NSCs led to a significant drop in CSF succinate at 30 dpt (Figure 1M; Table S1).

Further, we found no significant differences in CSF succinate when comparing PBS-treated EAE mice versus EAE mice injected icv with mouse fibroblasts (MFs) as control cells (Figure S3).

Thus, iNSCs and NSCs directly injected into the EAE CNS induce a specific phenotype switch of MPs, which is associated with reduction of the immunometabolite succinate in the CSF only and amelioration of chronic neuroinflammation.

NSCs Reduce Succinate Levels and Reprogram the Metabolism of Type 1 Inflammatory Mφ *In Vitro*

We then investigated the molecular mechanisms through which iNSCs/NSCs display anti-inflammatory activities on type 1 MPs, using an *in vitro* system that recapitulates the interactions between MPs and iNSCs/NSCs. Naive bone-marrow-derived macrophages (Mφ) were polarized into a type 1 inflammatory phenotype with LPS (Mφ^{LPS}), as described (Tannahill et al., 2013). Mφ^{LPS} were then co-cultured with iNSCs (Mφ^{LPS}-iNSCs) or NSCs (Mφ^{LPS}-NSCs) in a trans-well system that avoids cell-to-cell contacts (Figure 2A). Unpolarized Mφ were used as controls.

Microarray gene expression profiling showed significant transcriptional changes in Mφ^{LPS} with 7,401 genes affected (versus Mφ; adjusted p value < 0.1; Figure 2B; Table S2) and 51 genes differentially expressed in Mφ^{LPS}-iNSCs or Mφ^{LPS}-NSCs (versus

Figure 2. NSCs Reduce Succinate Levels and Reprogram the Metabolism of Type 1 Pro-inflammatory Mφ toward Oxidative Phosphorylation *In Vitro*

(A) Experimental setup for *in vitro* Mφ^{LPS} co-cultures with iNSCs/NSCs.

(B and C) Gene expression microarrays of Mφ^{LPS}-iNSCs/NSCs. (B) Venn diagram of differentially expressed genes (adjusted p value < 0.1). (C) Heatmap of genes differentially expressed (adjusted p value < 0.1) in Mφ^{LPS}-iNSCs or Mφ^{LPS}-NSCs.

(D and E) qRT-PCR independent validation of differentially expressed inflammatory genes as in (C). (D) Expression of genes related to type 1 inflammatory (E) and anti-inflammatory Mφ phenotypes relative to *Actb*. Data are mean fold change (±SEM) versus Mφ^{LPS} from n ≥ 3 independent replicates per condition.

(F) qRT-PCR of BV2^{LPS}-iNSCs/NSCs (±SEM) from n ≥ 3 independent experiments per condition. BV2 and BV2^{LPS} are shown as controls.

(G and H) Extracellular flux (XF) assay of the oxygen consumption rate (OCR) (G) and extracellular acidification rate (ECAR) (H) in Mφ^{LPS}-iNSCs/NSCs. Data were normalized on total protein content and are expressed as mean values (±SEM) from n ≥ 3 independent experiments per condition.

(I and J) Levels of significantly changed extracellular (*EXTRA_Metab*, I) and intracellular (*INTRA_Metab*, J) metabolites in Mφ^{LPS} versus Mφ at 25 hr. Data are mean a.u. (±SEM) from n ≥ 2 independent experiments per condition.

(K and L) Hif-1α (K), PKM2 (K), and IL-1β (L) expression levels relative to β-actin. Data are mean fold change versus Mφ^{LPS} (±SEM) from n ≥ 3 independent experiments per condition.

*p ≤ 0.05 and **p ≤ 0.01 versus Mφ^{LPS}. See also Tables S2 and S3.

$M\varphi^{LPS}$; adjusted p value < 0.1; Figures 2B and 2C; Table S2). This latter set of genes was enriched in biological processes related to positive regulation of leukocyte activation (GO: 0002696), myeloid leukocyte differentiation (GO: 0002761), and immune system processes (GO: 0002376). Independent qRT-PCR validation of selected Mφ pro-inflammatory genes confirmed significant downregulation of the expression levels of *Il12b*, *Il15*, *Il15ra*, and *Cd69*, as well as the classical inflammatory genes *Nos2*, *tumor necrosis factor* (*Tnf*), and *Il1b* in $M\varphi^{LPS}$-iNSCs and $M\varphi^{LPS}$-NSCs (versus $M\varphi^{LPS}$; Figure 2D). This effect was coupled with the concomitant upregulation of the expression levels of genes associated with an anti-inflammatory Mφ phenotype, such as uronyl-2-sulfotransferase (*Ust*) and *bone marrow stromal cell antigen 1* (*Bst1*) (Al-Shabany et al., 2016; Martinez et al., 2015), as well as *arginase 1* (*Arg1*) and *Mrc1* (versus $M\varphi^{LPS}$; Figure 2E). When iNSCs/NSCs were co-cultured with lipopolysaccharide (LPS)-activated mouse BV2 microglial cells as before, significant reduction of the expression levels of the pro-inflammatory genes *Nos2* and *Il1b* was also observed (Figure 2F).

To link gene expression profiles with functional metabolic states, we assessed the basal oxygen consumption rate (OCR) and extracellular acidification rate (ECAR) of $M\varphi^{LPS}$ as readouts of their tricarboxylic acid (TCA) cycle and glycolytic activities, respectively. We found a significant reduction of OCR and a significant increase of ECAR in $M\varphi^{LPS}$ (versus Mφs). Instead, $M\varphi^{LPS}$-iNSCs and $M\varphi^{LPS}$-NSCs underwent significant restoration of both OCR and ECAR values (versus $M\varphi^{LPS}$; Figures 2G and 2H), as observed in Mφ switching to an anti-inflammatory phenotype (O'Neill and Pearce, 2016).

In an effort to clarify the metabolic determinants of these anti-inflammatory effects, we performed an untargeted LC-MS analysis of the extracellular and intracellular small-molecule metabolite content of $M\varphi^{LPS}$. As expected, LPS stimulation profoundly changed the extracellular and intracellular metabolic milieu of Mφ ($M\varphi^{LPS}$) (versus Mφ; Table S3). In co-cultures, $M\varphi^{LPS}$-iNSCs and $M\varphi^{LPS}$-NSCs both showed significant reduction of extracellular glutamate, GABA, and succinate (versus $M\varphi^{LPS}$; Figure 2I; Table S3). Furthermore, $M\varphi^{LPS}$-iNSCs and $M\varphi^{LPS}$-NSCs also displayed a significant reduction of intracellular succinate and itaconate (versus $M\varphi^{LPS}$; Figure 2J; Table S3).

Consistent with the reduction of succinate levels, we found that $M\varphi^{LPS}$-iNSCs and $M\varphi^{LPS}$-NSCs exhibited significantly reduced levels of HIF-1α, of the upstream protein pyruvate kinase isozyme M2 (PKM2) (Palsson-McDermott et al., 2015; Figure 2K), as well as of IL-1β (versus $M\varphi^{LPS}$; Figure 2L).

Altogether, these *in vitro* data provide evidence that iNSCs/NSCs reduce the accumulation of both intracellular and extracellular succinate in co-cultures with type 1 inflammatory MPs, reprogramming them toward an OXPHOS anti-inflammatory phenotype.

Succinate Signals via SUCNR1/GPR91 in Mouse and Human NSCs

Given the importance of succinate as immunometabolic signal, we investigated whether succinate released by type 1 pro-inflammatory MPs could regulate the activity of surrounding cells *in situ*, including that of transplanted iNSCs/NSCs.

We found that transplanted iNSCs/NSCs detected in proximity to meningeal perivascular areas (Figures 3A and 3B) and $F4/80^+$ MPs (Figure 3C) expressed SUCNR1 *in vivo* in the CNS. SUCNR1 was also expressed at protein level on both iNSCs and NSCs *in vitro*, but not in MFs (Figure 3D).

To further assess whether SUCNR1 in iNSCs/NSCs was functionally activated by succinate, we investigated its downstream signaling cascade *in vitro*. When exposed to succinate (Figure 3E; Rubic et al., 2008), 34.2% (±7.4%) of iNSCs and 31.7% (±6.5%) of NSCs showed a release of intracellular calcium stores (Figures S4 and 3F). This response was followed by a significant upregulation of the phospho-p38 mitogen-activated protein kinase (Figure 3G), indicative of its activation. We confirmed the expression of *SUCNR1* and SUCNR1 also in human fetal NSCs (hNSCs) and human iNSCs (hiNSCs) (Figures 3H and 3I). As in mouse iNSCs, succinate-dependent p38 signaling was evoked in hiNSCs, but not in hiNSCs pre-treated with the selective SUCNR1 inhibitor *4c* (Figure 3J).

Thus, mouse and human iNSCs and NSCs express functional SUCNR1, which induces a signaling pathway downstream of its stimulation with the immunometabolite succinate.

SUCNR1 Stimulation Initiates the Secretion of Prostaglandin E2 by NSCs

To clarify the functional consequences of SUCNR1 signaling in NSCs, we generated NSCs from mice lacking *Sucnr1* (*Sucnr1*$^{-/-}$ NSCs) (Rubic et al., 2008; Figure S4). Compared to control NSCs, *Sucnr1*$^{-/-}$ NSCs showed similar growth curves and differentiation *in vitro* (Figure S4). However, when exposed to succinate at different time points and concentrations, *Sucnr1*$^{-/-}$ NSCs showed no upregulation of phospho-p38 (Figure S4). Stimulation with glutamate or ATP + thapsigargin induced in *Sucnr1*$^{-/-}$ NSCs a calcium response similar to that of control NSCs (Figure S4). On the contrary, succinate treatment did not elicit release of calcium from intracellular stores (Figure S4), which indicated a defective SUCNR1 signaling in *Sucnr1*$^{-/-}$ NSCs.

We then performed a gene expression profiling microarray following treatment with succinate in control NSCs and *Sucnr1*$^{-/-}$ NSCs (Table S4). We found that *prostaglandin-endoperoxide synthase 2* (*Ptgs2*), the key enzyme in PG biosynthesis encoding the inducible PTGS2, was the most upregulated gene in succinate-stimulated control NSCs ($\log_2$ fold change 1.05), but not in succinate-stimulated *Sucnr1*$^{-/-}$ NSCs ($\log_2$ fold change −0.43; Figure 4A). We validated these results on *Ptgs2* by qRT-PCR, confirming that its expression levels were significantly upregulated (2.1- to 2.7-fold change) in succinate-stimulated iNSCs and NSCs, whereas they were not in succinate-treated *Sucnr1*$^{-/-}$ NSCs (Figure 4B).

Given the role of PGE2 as regulator of the immunosuppressive effects of mesenchymal stem cells (MSCs) (Vasandan et al., 2016; Yañez et al., 2010), we tested its accumulation in tissue culture media from iNSCs, NSCs, and *Sucnr1*$^{-/-}$ NSCs after stimulation with succinate. iNSCs and NSCs, but not *Sucnr1*$^{-/-}$ NSCs, showed significant (>2.5-fold) increase of their basal release of PGE2 as early as 30 min after succinate. This succinate-induced effect was abolished by pre-treatment with the irreversible PTGS2 blocker SC-58125 (Figure 4C). As in mouse iNSCs, exposure of hiNSCs to succinate elicited a significant

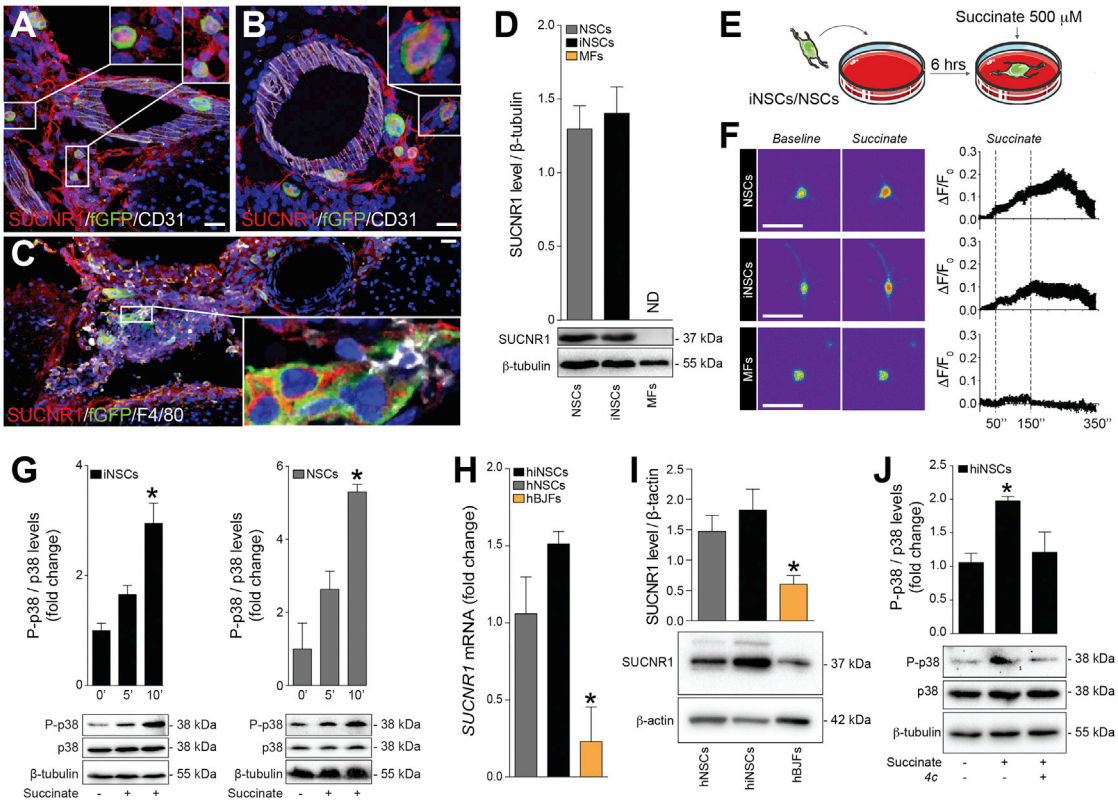

Figure 3. Succinate Signals via SUCNR1 in Mouse and Human NSCs

(A–C) Representative confocal microscopy images of meningeal perivascular areas with transplanted fGFP$^+$ iNSCs (A) and NSCs (B) expressing SUCNR1 in the brain of a mouse with EAE. The image in (C) shows transplanted SUCNR1$^+$ iNSCs in close vicinity to SUCNR1$^+$/F4/80$^+$ MPs. Nuclei are stained with DAPI.

(D) SUCNR1 protein expression relative to β-tubulin *in vitro*. Data are shown as mean (±SEM) of n ≥ 3 independent replicates per condition.

(E) Experimental setup for succinate treatment of iNSCs/NSCs *in vitro*.

(F) Intracellular Ca^{2+} response after treatment with 500 μM succinate (live staining with Fluo-4AM). Representative images (baseline and during stimulation) are pseudocolored with red/blue according to high/low fluorescence intensity. Data are mean changes in fluorescence intensity as ΔF/F0 (±SEM) from n ≥ 3 experiments.

(G) Phospho-p38 MAPK (P-p38) and total p38 MAPK (p38) protein expression after succinate treatment. Data are P-p38/p38 expression relative to β-tubulin and expressed as mean fold change (±SEM) versus untreated cells over n ≥ 3 independent experiments per condition.

(H) qRT-PCR of *SUCNR1* basal expression in human cells. Data are normalized on *18S* and expressed as mean fold change (±SEM) versus NSCs from n ≥ 3 independent replicates per condition.

(I) Representative blot of SUNCR1 basal protein expression in human cells.

(J) P-p38 and p38 protein expression after stimulation with succinate ± pre-treatment with the irreversible inhibitor of the human SUCNR1 *4c*.

The scale bars represent 25 μm. *p ≤ 0.05 versus 0'. hBJFs, human BJ fibroblasts; ND, not detected. See also Figure S4.

increase of PGE2 concentrations in tissue culture media, whereas again pre-treatment with either SC-58125 or *4c* prevented its release (Figure 4D).

To further extend the relevance of these findings to co-cultures between NSCs and Mφ^{LPS}, we analyzed the levels of PGE2 in tissue culture media. We found that Mφ^{LPS}-NSCs accumulated higher levels of PGE2 compared to Mφ^{LPS}, whereas pre-treatment of co-cultured NSCs with SC-58125 significantly reduced PGE2 levels (Figure 4E). SC-58125 pre-treatment of NSCs was also coupled with a significant increase of *Il1b* expression in Mφ^{LPS} (Figure 4F) and with a reduction of OCR values indicative of a pro-inflammatory phenotype (Figure 4G). However, we noticed that NSCs pre-treated with SC-58125 retained some residual anti-inflammatory effects on Mφ^{LPS} compared to *Sucnr1*$^{-/-}$ NSCs (Figure 4F). On the contrary, *Sucnr1* loss of function in NSCs completely abolished their anti-inflammatory effects on Mφ^{LPS} (Figures 4F and 4G). We also show that the observed PGE2-dependent anti-inflammatory ability of NSCs is conserved and relevant for human NSCs.

As such, hiNSCs induced a significant reduction of *Il1b* expression in Mφ^{LPS} in co-cultures (Figure 4H), which was coupled with a restoration of OCR values (Figure 4I) and increased PGE2 levels in tissue culture media (Figure 4J). These effects were completely suppressed by pre-treatment of hiNSCs with the selective SUCNR1 inhibitor *4c* (Figures 4H–4J).

Thus, the activation of SUCNR1 signaling pathway in mouse and human NSCs triggers the release of PGE2 leading to anti-inflammatory effects on type 1 MPs.

However, inhibition experiments targeting either PTGS2 or SUCNR1 anticipate that additional SUCNR1-dependent—PGE2-independent—mechanisms are likely to play a key role in the anti-inflammatory effects of NSCs.

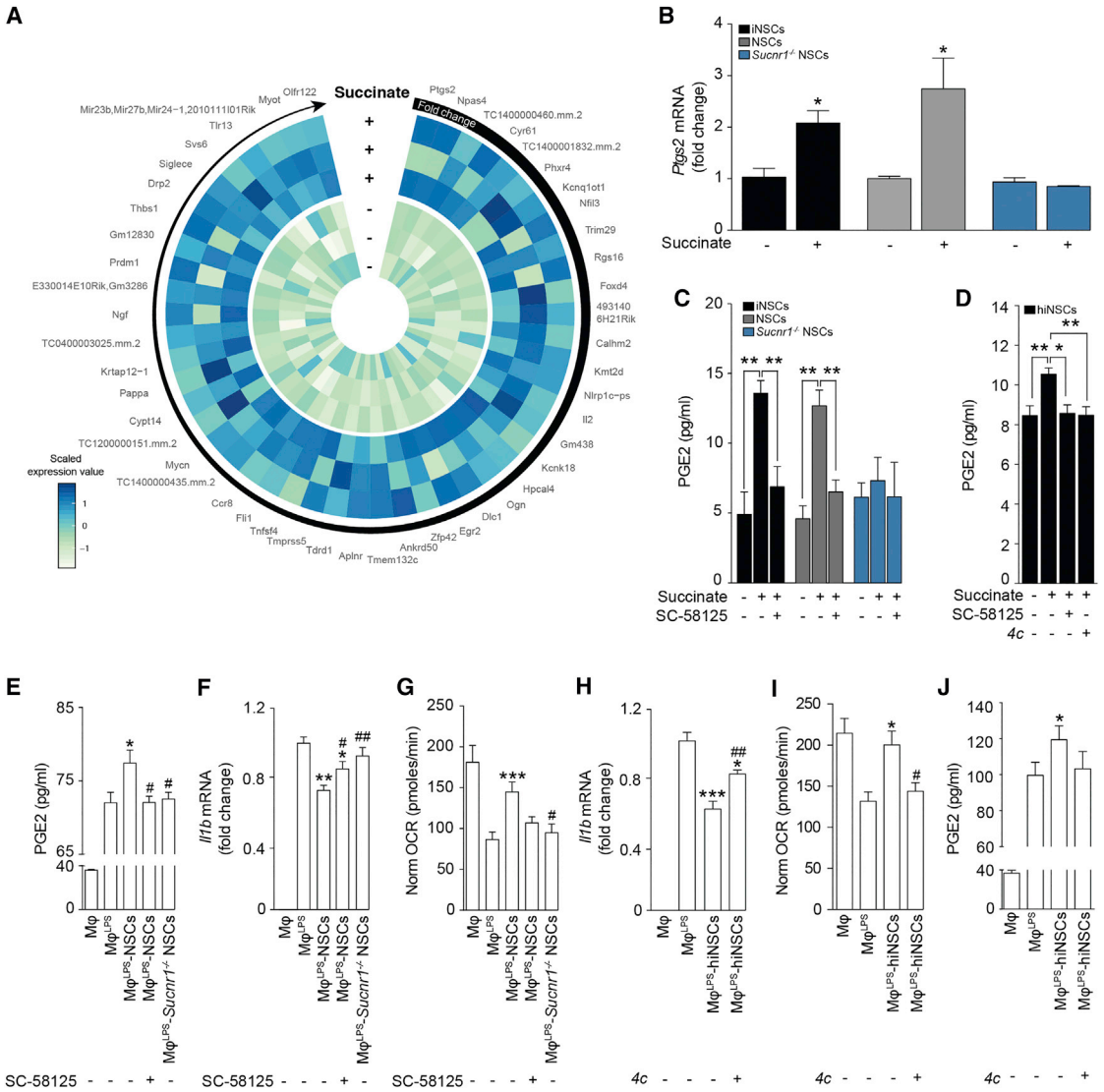

Figure 4. SUCNR1 Expression Is Necessary for the Anti-inflammatory Effect of NSCs on Type 1 Pro-inflammatory Mφ *In Vitro*

(A) Heatmap showing the microarray expression profile of the 50 most upregulated genes in NSCs after treatment with succinate. Data are shown as *Z* scores.

(B) qRT-PCR independent validation of *Ptgs2* expression as in (A). Data are calculated relative to *Actb* and shown as mean fold change (±SEM) versus untreated cells over n ≥ 3 independent experiments per condition.

(C) PGE2 secretion following 1 hr treatment with succinate ± pre-treatment with the selective PTGS2 blocker SC-58125. Data are mean values (±SEM) over n ≥ 3 independent experiments per condition.

(D) PGE2 secretion by hiNSCs treated with succinate ± pre-treatment with either SC-58125 or *4c*. Data are mean values (±SEM) over n ≥ 3 independent experiments per condition.

(E) PGE2 secretion in Mφ co-cultures. Data are mean values (±SEM) over n ≥ 3 independent experiments per condition.

(F) *Il1b* expression relative to *Actb* in Mφ co-cultures. Data are mean fold change versus $M\varphi^{LPS}$ (±SEM) from n ≥ 3 independent experiments per condition.

(G) XF assay of the OCR of Mφ as in (E) and (F). Data are normalized on total protein content and expressed as mean values (±SEM) over n ≥ 3 independent experiments per condition.

(H) *Il1b* expression relative to *Actb* of Mφ co-cultures with hiNSCs. Data are mean fold change versus $M\varphi^{LPS}$ (±SEM) from n ≥ 3 independent experiments per condition.

(I) XF assay showing the OCR of Mφ as in (H). Data are normalized on total protein content and expressed as mean values (±SEM) over n ≥ 2 independent experiments per condition.

(J) PGE2 secretion in Mφ co-cultures as in (H) and (I). Data are mean values (±SEM) over n ≥ 3 independent experiments per condition.

*p ≤ 0.05 versus untreated cells (B); *p ≤ 0.05 and **p ≤ 0.01 (C and D); *p ≤ 0.05, **p ≤ 0.01, and ***p ≤ 0.001 versus $M\varphi^{LPS}$ (E–J); #p ≤ 0.05 and ##p ≤ 0.01 versus $M\varphi^{LPS}$-NSCs (E–G) or versus $M\varphi^{LPS}$-hiNSCs (H and I). See also Figure S4 and Table S4.

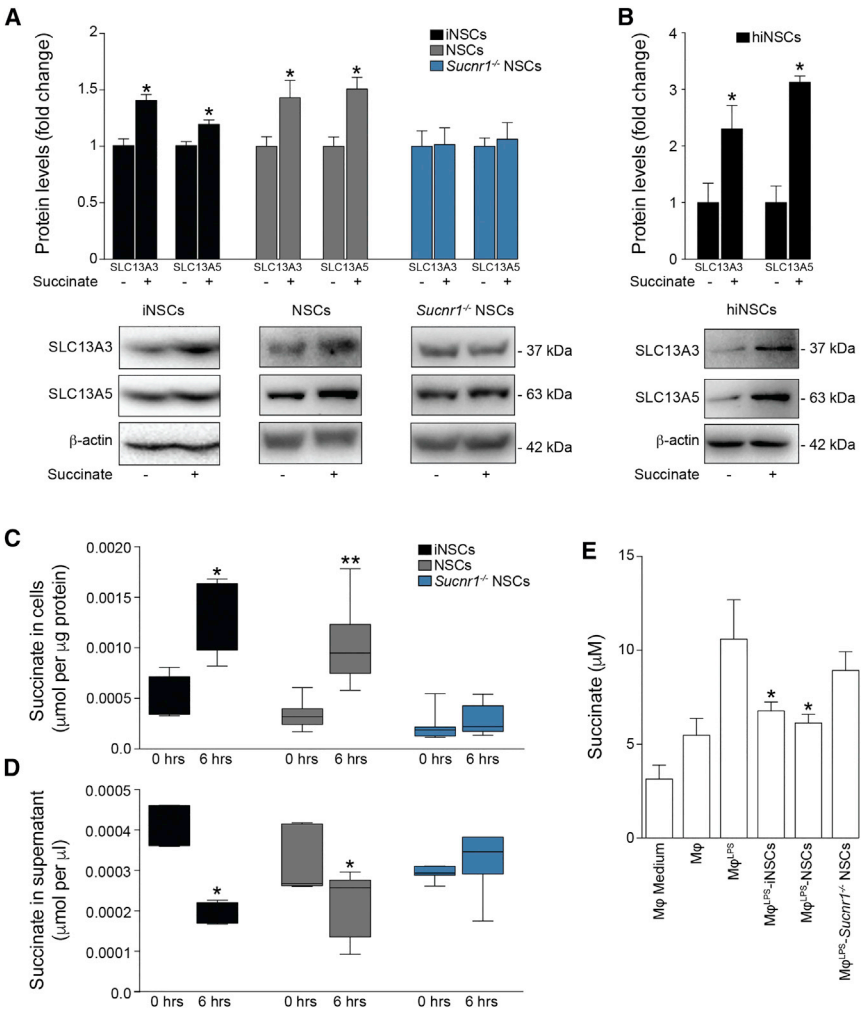

Figure 5. SUCNR1 Regulates the Uptake of Succinate by NSCs *In Vitro*

(A) SLC13A3 and SLC13A5 protein expression levels after 2 hr of succinate treatment.

(B) SLC13A3 and SLC13A5 protein expression levels after 6 hr of succinate treatment in hiNSCs. Data in (A) and (B) are relative to β-actin and expressed as mean fold change (±SEM) versus untreated cells over n ≥ 3 independent experiments per condition.

(C and D) Uptake assay of [^{14}C]-labeled succinate at 0 and 6 hr. (C) Intracellular [^{14}C] labeling and (D) extracellular [^{14}C] signal in tissue culture media are shown. Box-whiskers plots ± min to max value from n ≥ 4 technical replicates per group from n = 2 independent experiments are shown.

(E) Succinate release in Mφ co-cultures. Data are mean values versus Mφ (±SEM) from n ≥ 2 independent experiments per condition.

*p ≤ 0.05 versus untreated cells (A and B) or versus Mφ^{LPS} (E); *p ≤ 0.05 and **p ≤ 0.01 versus 0 hr, Mann-Whitney test (C and D). See also Figure S5.

SUCNR1 Stimulation Triggers the Uptake of Succinate by NSCs

Gene expression arrays of succinate-stimulated NSCs revealed that, besides *Ptgs2*, *NaCT/Slc13a5* was among the most upregulated genes in wild-type (WT) NSCs (log_2 fold change = 0.49), but not in *Sucnr1*$^{-/-}$ NSCs (log_2 fold change = −0.12). SLC13A5 is a dicarboxylate co-transporter known to be involved in succinate transport (Srisawang et al., 2007). Given the consistent depletion of succinate found both *in vivo* in the CSF of iNSC- or NSC-transplanted EAE mice and *in vitro* in co-cultures with Mφ^{LPS}, we hypothesized that iNSCs/NSCs would activate SLC13A5 to scavenge succinate.

We found that the expression of SLC13A5, as well as of the high-affinity dicarboxylate co-transporter SLC13A3, were significantly increased in iNSCs and NSCs, but not in *Sucnr1*$^{-/-}$ NSCs, upon succinate stimulation (Figure 5A). Similarly, hiNSCs exposed to succinate upregulated the protein expression levels of both these SLC13 co-transporters *in vitro* (Figure 5B).

We next investigated the role of these co-transporters by measuring succinate uptake in iNSCs and NSCs. We found that both iNSCs and NSCs significantly accumulated [^{14}C]-succinate (Figure 5C) while reducing the amount of extracellular [^{14}C]-succinate in tissue culture media (Figure 5D). *Sucnr1*$^{-/-}$ NSCs neither accumulated [^{14}C]-succinate intracellularly nor did they deplete it extracellularly (Figures 5C and 5D). Interestingly, *Sucnr1*$^{-/-}$ NSCs, which we have shown to have no effects on *Il1b* expression in Mφ^{LPS} (Figure 4F), failed to reduce the extracellular succinate levels in co-cultures with Mφ^{LPS} (Figure 5E). As further proof of the importance of succinate depletion in modulating the phenotype of type 1 pro-inflammatory MPs, we show that treatment with active recombinant (r)SDH complex subunit A is able to significantly reduce the expression of *Il1b* in Mφ^{LPS} (Figure S5).

Thus, SUCNR1 signaling in NSCs prompts the uptake of the immunometabolite succinate, thereby depleting the available extracellular pool sustaining the autocrine and paracrine activation of type 1 MPs.

Transplantation of *Sucnr1* Loss-of-Function NSCs Shows Impaired Ability to Ameliorate Chronic Neuroinflammation *In Vivo*

To confirm the role of the succinate-SUCNR1 axis in mediating the response of NSC grafts to succinate *in vivo*, we assessed the effects of the icv transplantation of *Sucnr1*$^{-/-}$ NSCs in mice with chronic EAE.

At 30 dpt, *Sucnr1*$^{-/-}$ NSCs survived, distributed, and integrated within the EAE brain and spinal cord with no significant differences compared to control NSCs (Figure S6). However, the transplantation of *Sucnr1*$^{-/-}$ NSCs induced only a slight recovery of EAE behavioral deficits versus PBS-treated control EAE mice (EAE score—*Sucnr1*$^{-/-}$ NSCs: 2.9 ± 0.2; PBS: 3.6 ± 0.4), which was significantly less pronounced (50% of the effect) than that observed in EAE mice transplanted with control NSCs (EAE score—NSCs: 2.1 ± 0.3; Figure 6A).

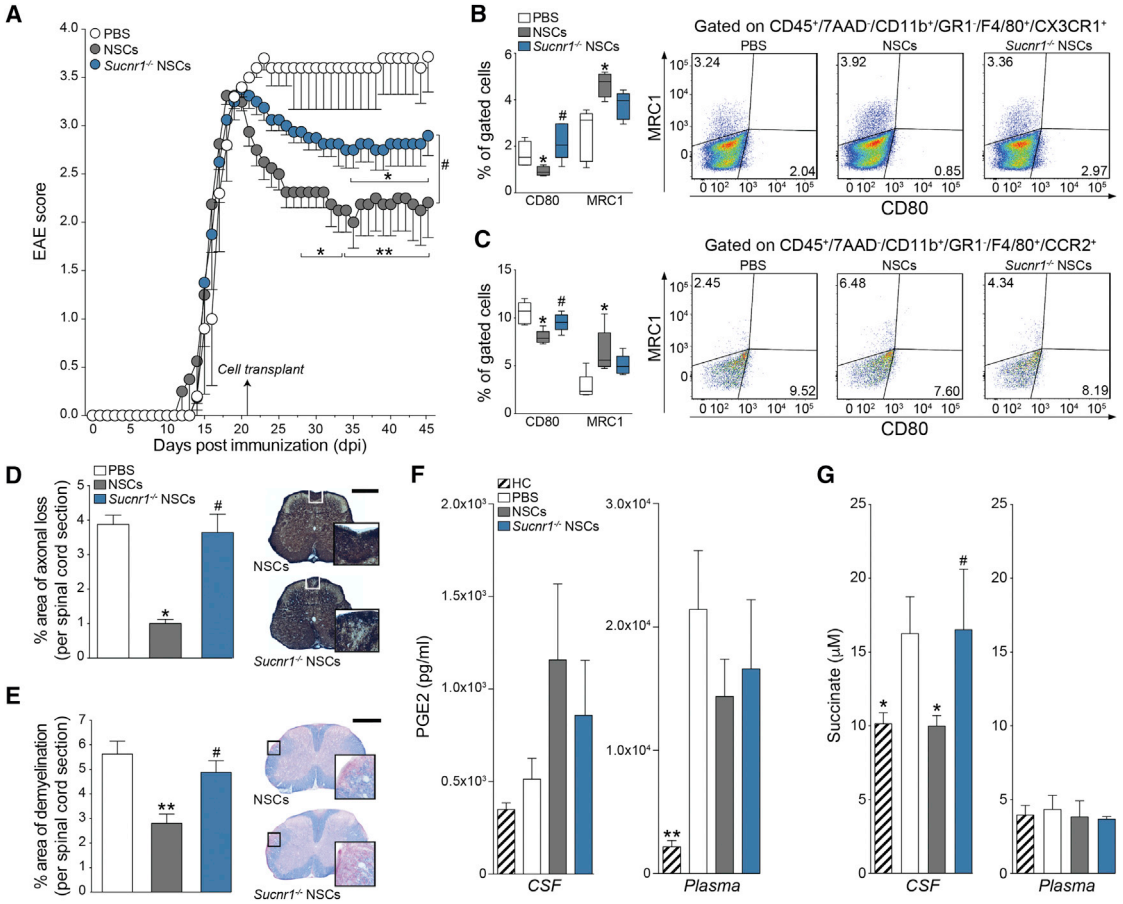

Figure 6. Transplantation of *Sucnr1* Loss-of-Function NSCs Shows Impaired Ability to Ameliorate Chronic Neuroinflammation *In Vivo*

(A) Behavioral outcome of EAE mice. Data are mean EAE score (±SEM) from n ≥ 5 mice/group.

(B and C) Flow-cytometry-based *ex vivo* quantification of the expression levels of type 1 inflammatory (CD80) and anti-inflammatory (MRC1) markers in CX3CR1$^+$ microglial cells (B) and CCR2$^+$ monocyte-derived infiltrating macrophages (C) at 30 dpt. Quantitative data are shown on the left, whereas representative density plots are shown on the right. Data are min to max % of marker-positive cells from n ≥ 4 pools of mice/group.

(D and E) Pathological outcomes of experiments as in (A). Data are mean % Bielschowsky negative-stained axonal loss (D) or LFB negative-stained demyelinated (E) areas/spinal cord section (±SEM) from n ≥ 4 mice/group. The scale bars represent 400 μm.

(F) PGE2 levels in the CSF and plasma of EAE mice at 30 dpt. Data are mean values (±SEM) from n ≥ 3 samples/group.

(G) Succinate levels in the CSF and plasma of EAE mice at 30 dpt. Data are mean values (±SEM) from n ≥ 4 mice/group. Kruskal-Wallis followed by Mann-Whitney post-test is shown.

*p ≤ 0.05, **p ≤ 0.01, and ***p ≤ 0.001 versus PBS; #p ≤ 0.05 versus NSCs. See also Figure S6.

Ex vivo flow-cytometry-based analysis of the composition of CNS inflammatory infiltrates showed that transplantation of EAE mice with *Sucnr1*$^{-/-}$ NSCs failed to shift the proportions of type 1 inflammatory and anti-inflammatory MPs—including CX3CR1$^+$ microglia and CCR2$^+$ monocyte-derived infiltrating macrophages—in contrast with the effects of control NSCs (Figures 6B and 6C). *Post mortem* tissue pathology further confirmed the reduced tissue-protective effects of *Sucnr1*$^{-/-}$ NSC grafts (Figures 6D and 6E).

We then investigated the levels of PGE2 and succinate in matched CSF and plasma samples from NSC-transplanted and PBS-treated control EAE mice. We found that both *Sucnr1*$^{-/-}$ NSCs and control NSCs failed to induce significant changes of the levels of PGE2 in the CSF. Plasma PGE2 significantly increased in EAE mice only (versus healthy controls), with no treatment effect observed (Figure 6F). Importantly, whereas transplantation of control NSCs reduced CSF succinate (HC: 5.524 × 10^7 a.u. ± 0.19; PBS: 9.35 × 10^7 a.u. ± 0.14; NSCs: 5.64 × 10^7 a.u. ± 0.44), *Sucnr1*$^{-/-}$ NSC grafts showed no effects (*Sucnr1*$^{-/-}$ NSCs: 10.40 × 10^7 a.u. ± 2.59; Figure 6G).

These data confirm the requirement of a functional SUCNR1 signaling pathway in the regulation of the anti-inflammatory and neuroprotective effects of NSC transplants *in vivo* and underline the importance of succinate scavenging as a predominant anti-inflammatory mechanism of action of NSCs.

DISCUSSION

There is an unmet clinical need to develop cellular and molecular approaches to target core drivers of the pathophysiology of chronic neuroinflammatory conditions that include progressive forms of MS (Volpe et al., 2016). In principle, stem cells possess

a therapeutic potential that is distinct from that of small molecules and biologics and extend far beyond the classical regenerative medicine arena. Part drug and part device, stem cells could work as biological disease-modifying agents (DMAs) that sense diverse signals, migrate to specific sites in the body, integrate inputs to make decisions, and execute complex response behaviors in the context of a specific tissue microenvironment (Fischbach et al., 2013). All these attributes could be harnessed to treat several disease processes, including the persistent MP-driven inflammation and tissue degeneration that occur in progressive MS.

Here, we used accessible, autologous, and stably expandable iNSCs (Thier et al., 2012), as well as somatic NSCs, to investigate the effects of brain stem cell transplantation in a mouse model of chronic neuroinflammation, which mimics the inflammatory cascade observed in progressive MS.

We found that the transplantation of iNSCs into the CSF circulation of EAE mice promotes equivalent outcomes to those previously observed in mice transplanted with somatic NSCs (Pluchino et al., 2003). Transplanted iNSCs or NSCs induced significant clinical amelioration, as well as reduced axonal and myelin damage, with no significant reduction of BBB permeability at 30 dpt. Further studies will help clarify whether changes of BBB permeability or recruitment of inflammatory monocytes to the CNS occur immediately following the transplantation of iNSCs/NSCs. Whether such an effect is likely to change the main clinical outcomes of diseases with high prevalence of CNS infiltration by inflammatory cells, such as EAE/MS, is hard to anticipate.

Instead, we found that our paradigm of transplantation was associated with a specific switch in the activation profile of both $CX3CR1^{+}$ microglial cells and $CCR2^{+}$ monocyte-derived infiltrating macrophages with a decrease of the $CD80^{+}$ type 1 inflammatory MPs and parallel increase of the $MRC1^{+}$ anti-inflammatory MPs. Transplanted iNSCs/NSCs distributed and survived in the CNS of EAE mice, while preferentially accumulating at the level of meningeal perivascular areas in juxtaposition to endogenous MPs. Altogether, these findings would imply the presence of some yet unknown mechanisms of intercellular coupling between grafted stem cells and inflammatory MPs. Whether this iNSC/NSC-MP communication *in vivo* takes place only in perivascular niches or also at the level of other emerging immune sensor-like structures of the brain that include the choroid plexus remains to be addressed (Ge et al., 2017).

We then investigated the underlying immunological mechanisms driving the beneficial effects of NSCs on MPs during chronic neuroinflammation. Untargeted small molecule analysis of matched CSF and plasma samples revealed profound metabolic changes in the CSF of EAE mice, with differences between the early and the delayed phases of disease.

Carnitine, leucine + isoleucine, citrulline, allantoin, ornithine, and uric acid were all significantly increased in the PBS-treated control EAE mice at the peak of disease. Our findings are consistent with published evidence showing that leucine, as well as uric acid and its by-product allantoin, are all increased in the CSF of subjects with MS (Amorini et al., 2009; Hooper et al., 1998; Monaco et al., 1979). Whereas increased CSF carnitine has not been reported in MS, important increases have been described in non-MS inflammatory conditions of the CNS, such as encephalitis (Wikoff et al., 2008) and meningitis (Shinawi et al., 1998).

Conversely, only succinate showed a delayed (i.e., 45 dpi) increase in the CSF of PBS-treated control EAE mice. Succinate is becoming a valuable *in vivo* biomarker of metabolic distress and inflammatory activity (Littlewood-Evans et al., 2016; Mills and O'Neill, 2014). Importantly, we found that succinate was significantly decreased in the CSF of iNSC-/NSC-transplanted mice. The reduction of CSF succinate following iNSC or NSC transplantation was of interest and might have a prominent role in interfering with chronic neuroinflammation.

Succinate released from type 1 inflammatory MPs is a key inflammatory signal that interacts with its specific G-protein-coupled receptor SUCNR1. SUCNR1 acts as an early detector of metabolic stress in several physiological and pathological conditions, including renin-induced hypertension, ischemia/reperfusion injury, inflammation, platelet aggregation, and retinal angiogenesis (de Castro Fonseca et al., 2016; Gilissen et al., 2016). Notably, we found that the expression of SUCNR1 is required for the therapeutic effects of transplanted NSCs *in vivo*.

Succinate-mediated activation of SUCNR1 on rodent and human iNSCs and NSCs activates calcium signaling and mitogen-activated protein kinase (MAPK) phosphorylation *in vitro*, thus eliciting the acquisition of a concerted anti-inflammatory phenotype in NSCs. On the one hand, SUCNR1 activated the secretion of PGE2, a well-established pleiotropic immune modulator, whose function targets multiple cell types within the inflamed microenvironment, including MPs (Kota et al., 2017; Vasandan et al., 2016). On the other hand, succinate-SUCNR1 signaling in iNSCs and NSCs led to the upregulation of two members of the SLC13 family of co-transporters (i.e., SLC13A3 and SLC13A5) and uptake of extracellular succinate.

In vivo, we demonstrate effective scavenging of extracellular local succinate by NSCs injected in EAE mice through the CSF circulation, which is predominant, compared to the secretion of PGE2. The loss of SUCNR1-dependent signaling in transplanted NSCs led to significant reduction in their anti-inflammatory and neuroprotective effects, whereas *Sucnr1*$^{-/-}$ NSC grafts showed no difference of survival, distribution, and differentiation versus control NSCs.

We then hypothesize that the extracellular succinate secreted by type 1 inflammatory MPs initiates a scavenging behavior that transplanted NSCs adjust in response to increased substrate availability (Srisawang et al., 2007). This novel intercellular metabolic coupling fits well with the available literature showing that, within specific microenvironments, cells compete for available nutrients, affecting each other's function and fate (Pearce and Pearce, 2013).

We anticipate that succinate depletion by SUCNR1-expressing iNSCs and NSCs might play a crucial role in reducing the availability of a key metabolic signal in inflammatory contexts where the interactions between transplanted stem cells and host immune cells become complementary (Pluchino and Cossetti, 2013). More generally, our findings are in line with the provocative, yet still emerging, concept of NSCs as ancestral guardians of the brain capable of exerting several complementary immune modulatory and tissue trophic effects (Martino and Pluchino, 2007).

Additional studies are needed to further characterize the function of the succinate-SUCNR1 axis in neuro-immune interactions, provide additional insights on the critical role of cellular

metabolism for neural stem/progenitor cells (Knobloch and Jessberger, 2017), and develop complementary pharmacological interventions targeting this pathway in the chronically inflamed brain.

In conclusion, we show here that NSCs sense the extracellular succinate that accumulates in the chronically inflamed CNS to ameliorate neuroinflammation via succinate-SUCNR1-dependent mechanisms. Our work identifies a novel anti-inflammatory mechanism that underpins the regenerative potential of somatic and directly induced NSCs, thus paving the way for a new era of personalized stem cell medicines for chronic inflammatory and degenerative neurological diseases.

STAR★METHODS

Detailed methods are provided in the online version of this paper and include the following:

- KEY RESOURCES TABLE
- CONTACT FOR REAGENT AND RESOURCE SHARING
- EXPERIMENTAL MODEL AND SUBJECT DETAILS
- METHOD DETAILS
  - Mouse iNSC/NSC proliferation, viability and differentiation *in vitro*
  - Fluorescence-activated cell sorting (FACS) analysis
  - Type-1 inflammatory Mφ or BV2 cells co-cultures with iNSCs/NSCs
  - Recombinant SDHA activity and treatment of type-1 inflammatory Mφ
  - Lentiviral fGFP tagging
  - EAE induction, transplantation and behavioral studies
  - *Ex vivo* tissue pathology
  - Blood brain barrier functional analysis
  - Plasma and cerebrospinal fluid (CSF) sampling
  - Calcium imaging
  - ELISA
  - Uptake experiments with [^{14}C] - labeled succinate
  - Immunoblotting
  - Extracellular flux (XF) assays
  - Gene expression analysis (microarrays and qRT-PCR)
  - Metabolite extraction and LC-MS analysis
- QUANTITATION AND STATISTICAL ANALYSES
- DATA AND SOFTWARE AVAILABILITY

SUPPLEMENTAL INFORMATION

Supplemental Information includes six figures and four tables and can be found with this article online at https://doi.org/10.1016/j.stem.2018.01.020.

ACKNOWLEDGMENTS

The authors thank P. Chinnery, F. Dazzi, D. Franciotta, J. Jones, A. Tolkovsky, and L. Vallier for critically discussing the article. The authors wish to acknowledge G. Pluchino, J. Smith, G. Tannahil, and K. Saeb-Parsy for their technical contributions and critical insights throughout the execution of the study and A. Elkalhoun and W. Wu of the NIH/NHGRI IRP Microarray Core Facility for their assistance with the transcriptomic/microarray studies. The authors also thank J.M. Carballido (Novartis, Switzerland) for providing the C57BL/6 *Sucnr1*$^{-/-}$ mice, A.L. Vescovi (Milano, Italy) for providing the RNA and protein extracts from human fetal NSCs (hNSCs), and S. De (Advinus Therapeutics TATA Enterprise, India) for providing the compound *4c* used in this study. This work was funded by the Italian Multiple Sclerosis Association (AISM) (grant 2010/R/31 and grant 2014/PMS/4 to S.P.), the United States Department of Defense (DoD) Congressionally Directed Medical Research Programs (CDMRP) (grant MS140019 to S.P.), the Italian Ministry of Health (GR08-7 to S.P.), the European Research Council (ERC) under the ERC-2010-StG grant agreement no. 260511-SEM_SEM, the Medical Research Council, the Engineering and Physical Sciences Research Council, the Biotechnology and Biological Sciences Research Council UK Regenerative Medicine Platform Hub "Acellular Approaches for Therapeutic Delivery" (MR/K026682/1 to S.P.), the Evelyn Trust (RG 69865 to S.P.) and the Bascule Charitable Trust (RG 75149 to S.P.). L.P.-J. was supported by a research training fellowship from the Wellcome Trust (RRZA/057 RG79423). J.D.B. was supported by a NIH-OxCam training fellowship. Work in the F.E. lab was supported by grants from the ERA-Net E-rare research programme and the Austrian Science Fund (FWF). C.K.K. was supported by a stipend of the German Excellence Initiative to the Graduate School of Life Sciences, University of Würzburg. J.M.H. was supported by the Intramural Research Program (IRP) of NINDS/NIH. Work in M.P.M.'s lab was supported by grants from the Medical Research Council UK (MC_U105663142) and by a Wellcome Trust Investigator award (110159/Z/15/Z).

AUTHOR CONTRIBUTIONS

Conceptualization, L.P.J., C.F., and S.P.; Methodology, L.P.J., F.E., and S.P.; Formal Analysis, L.P.J., J.D.B., N.V., A.S.H.C., T.L., C.F., and S.P.; Investigation, L.P.J., J.D.B., N.V., I.B., A.S.H.C., C.K.K., B.B., G. Mallucci, G. Manferrari., G.V., M.D., N.I., A.B., and L.M.B.; Resources, M.P.M., J.H., F.E., C.F., and S.P.; Data Curation, L.P.J., J.D.B., and N.V.; Writing – Original Draft, L.P.J., J.D.B., N.V., C.F., and S.P.; Writing – Review & Editing, L.P.J., J.D.B., N.V., M.P.M., J.H., F.E., C.F., and S.P.; Supervision, M.P.M., J.H., F.E., C.F., and S.P.; Project Administration, L.P.J., J.D.B., N.V., C.F., and S.P.; Funding Acquisition, L.P.J. and S.P.

DECLARATION OF INTERESTS

S.P. owns >5% of CITC.

Received: April 14, 2017
Revised: September 18, 2017
Accepted: January 25, 2018
Published: February 22, 2018

REFERENCES

Al-Shabany, A.J., Moody, A.J., Foey, A.D., and Billington, R.A. (2016). Intracellular NAD+ levels are associated with LPS-induced TNF-α release in pro-inflammatory macrophages. Biosci. Rep. *36*, e00301.

Amorini, A.M., Petzold, A., Tavazzi, B., Eikelenboom, J., Keir, G., Belli, A., Giovannoni, G., Di Pietro, V., Polman, C., D'Urso, S., et al. (2009). Increase of uric acid and purine compounds in biological fluids of multiple sclerosis patients. Clin. Biochem. *42*, 1001–1006.

Anderson, A.J., Piltti, K.M., Hooshmand, M.J., Nishi, R.A., and Cummings, B.J. (2017). Preclinical efficacy failure of human CNS-derived stem cells for use in the pathway study of cervical spinal cord injury. Stem Cell Reports *8*, 249–263.

Bacigaluppi, M., Pluchino, S., Peruzzotti-Jametti, L., Kilic, E., Kilic, U., Salani, G., Brambilla, E., West, M.J., Comi, G., Martino, G., and Hermann, D.M. (2009). Delayed post-ischaemic neuroprotection following systemic neural stem cell transplantation involves multiple mechanisms. Brain *132*, 2239–2251.

Bacigaluppi, M., Russo, G.L., Peruzzotti-Jametti, L., Rossi, S., Sandrone, S., Butti, E., De Ceglia, R., Bergamaschi, A., Motta, C., Gallizioli, M., et al. (2016). Neural stem cell transplantation induces stroke recovery by upregulating glutamate transporter GLT-1 in astrocytes. J. Neurosci. *36*, 10529–10544.

Bramow, S., Frischer, J.M., Lassmann, H., Koch-Henriksen, N., Lucchinetti, C.F., Sørensen, P.S., and Laursen, H. (2010). Demyelination versus remyelination in progressive multiple sclerosis. Brain *133*, 2983–2998.

Carvalho, B.S., and Irizarry, R.A. (2010). A framework for oligonucleotide microarray preprocessing. Bioinformatics *26*, 2363–2367.

Cusimano, M., Biziato, D., Brambilla, E., Donegà, M., Alfaro-Cervello, C., Snider, S., Salani, G., Pucci, F., Comi, G., Garcia-Verdugo, J.M., et al. (2012). Transplanted neural stem/precursor cells instruct phagocytes and reduce secondary tissue damage in the injured spinal cord. Brain *135*, 447–460.

de Castro Fonseca, M., Aguiar, C.J., da Rocha Franco, J.A., Gingold, R.N., and Leite, M.F. (2016). GPR91: expanding the frontiers of Krebs cycle intermediates. Cell Commun. Signal. *14*, 3.

Eftaxiopoulou, T., Macdonald, W., Britzman, D., and Bull, A.M.J. (2014). Gait compensations in rats after a temporary nerve palsy quantified using temporo-spatial and kinematic parameters. Journal of Neuroscience Methods *232*, 16–23.

Fischbach, M.A., Bluestone, J.A., and Lim, W.A. (2013). Cell-based therapeutics: the next pillar of medicine. Sci. Transl. Med. *5*, 179ps7.

Ge, R., Tornero, D., Hirota, M., Monni, E., Laterza, C., Lindvall, O., and Kokaia, Z. (2017). Choroid plexus-cerebrospinal fluid route for monocyte-derived macrophages after stroke. J. Neuroinflammation *14*, 153.

Gilissen, J., Jouret, F., Pirotte, B., and Hanson, J. (2016). Insight into SUCNR1 (GPR91) structure and function. Pharmacol. Ther. *159*, 56–65.

Grupp, C., and Müller, G.A. (1999). Renal fibroblast culture. Exp. Nephrol. *7*, 377–385.

Hooper, D.C., Spitsin, S., Kean, R.B., Champion, J.M., Dickson, G.M., Chaudhry, I., and Koprowski, H. (1998). Uric acid, a natural scavenger of peroxynitrite, in experimental allergic encephalomyelitis and multiple sclerosis. Proc. Natl. Acad. Sci. USA *95*, 675–680.

Jiang, Z., Jiang, J.X., and Zhang, G.X. (2014). Macrophages: a double-edged sword in experimental autoimmune encephalomyelitis. Immunol. Lett. *160*, 17–22.

Kelly, B., and O'Neill, L.A. (2015). Metabolic reprogramming in macrophages and dendritic cells in innate immunity. Cell Res. *25*, 771–784.

Knobloch, M., and Jessberger, S. (2017). Metabolism and neurogenesis. Curr. Opin. Neurobiol. *42*, 45–52.

Kota, D.J., Prabhakara, K.S., Toledano-Furman, N., Bhattarai, D., Chen, Q., DiCarlo, B., Smith, P., Triolo, F., Wenzel, P.L., Cox, C.S., Jr., et al. (2017). Prostaglandin E2 indicates therapeutic efficacy of mesenchymal stem cells in experimental traumatic brain injury. Stem Cells *35*, 1416–1430.

Littlewood-Evans, A., Sarret, S., Apfel, V., Loesle, P., Dawson, J., Zhang, J., Muller, A., Tigani, B., Kneuer, R., Patel, S., et al. (2016). GPR91 senses extracellular succinate released from inflammatory macrophages and exacerbates rheumatoid arthritis. J. Exp. Med. *213*, 1655–1662.

Liu, L., and Duff, K. (2008). A technique for serial collection of cerebrospinal fluid from the cisterna magna in mouse. J. Vis. Exp. (21), 960.

Lu, J., Liu, H., Huang, C.T., Chen, H., Du, Z., Liu, Y., Sherafat, M.A., and Zhang, S.C. (2013). Generation of integration-free and region-specific neural progenitors from primate fibroblasts. Cell Rep. *3*, 1580–1591.

Mallucci, G., Peruzzotti-Jametti, L., Bernstock, J.D., and Pluchino, S. (2015). The role of immune cells, glia and neurons in white and gray matter pathology in multiple sclerosis. Prog. Neurobiol. *127-128*, 1–22.

Martinez, P., Denys, A., Delos, M., Sikora, A.S., Carpentier, M., Julien, S., Pestel, J., and Allain, F. (2015). Macrophage polarization alters the expression and sulfation pattern of glycosaminoglycans. Glycobiology *25*, 502–513.

Martino, G., and Pluchino, S. (2006). The therapeutic potential of neural stem cells. Nat. Rev. Neurosci. *7*, 395–406.

Martino, G., and Pluchino, S. (2007). Neural stem cells: guardians of the brain. Nat. Cell Biol. *9*, 1031–1034.

Masters, S.L., Dunne, A., Subramanian, S.L., Hull, R.L., Tannahill, G.M., Sharp, F.A., Becker, C., Franchi, L., Yoshihara, E., Chen, Z., et al. (2010). Activation of the NLRP3 inflammasome by islet amyloid polypeptide provides a mechanism for enhanced IL-1β in type 2 diabetes. Nat. Immunol. *11*, 897–904.

Mazzini, L., Gelati, M., Profico, D.C., Sgaravizzi, G., Projetti Pensi, M., Muzi, G., Ricciolini, C., Rota Nodari, L., Carletti, S., Giorgi, C., et al. (2015). Human neural stem cell transplantation in ALS: initial results from a phase I trial. J. Transl. Med. *13*, 17.

Meyer, S., Wörsdörfer, P., Günther, K., Thier, M., and Edenhofer, F. (2015). Derivation of adult human fibroblasts and their direct conversion into expandable neural progenitor cells. J. Vis. Exp. *101*, e52831.

Mills, E., and O'Neill, L.A. (2014). Succinate: a metabolic signal in inflammation. Trends Cell Biol. *24*, 313–320.

Mills, E.L., Kelly, B., Logan, A., Costa, A.S.H., Varma, M., Bryant, C.E., Tourlomousis, P., Dabritz, J.H.M., Gottlieb, E., Latorre, I., et al. (2016). Succinate dehydrogenase supports metabolic repurposing of mitochondria to drive inflammatory macrophages. Cell *167*, 457–470.e13.

Moll, N.M., Rietsch, A.M., Thomas, S., Ransohoff, A.J., Lee, J.C., Fox, R., Chang, A., Ransohoff, R.M., and Fisher, E. (2011). Multiple sclerosis normal-appearing white matter: pathology-imaging correlations. Ann. Neurol. *70*, 764–773.

Monaco, F., Fumero, S., Mondino, A., and Mutani, R. (1979). Plasma and cerebrospinal fluid tryptophan in multiple sclerosis and degenerative diseases. J. Neurol. Neurosurg. Psychiatry *42*, 640–641.

O'Neill, L.A., and Pearce, E.J. (2016). Immunometabolism governs dendritic cell and macrophage function. J. Exp. Med. *213*, 15–23.

Orihuela, R., McPherson, C.A., and Harry, G.J. (2016). Microglial M1/M2 polarization and metabolic states. Br. J. Pharmacol. *173*, 649–665.

Palsson-McDermott, E.M., Curtis, A.M., Goel, G., Lauterbach, M.A., Sheedy, F.J., Gleeson, L.E., van den Bosch, M.W., Quinn, S.R., Domingo-Fernandez, R., Johnston, D.G., et al. (2015). Pyruvate kinase M2 regulates Hif-1α activity and IL-1β induction and is a critical determinant of the warburg effect in LPS-activated macrophages. Cell Metab. *21*, 65–80.

Pearce, E.L., and Pearce, E.J. (2013). Metabolic pathways in immune cell activation and quiescence. Immunity *38*, 633–643.

Peterson, J.W., Bö, L., Mörk, S., Chang, A., and Trapp, B.D. (2001). Transected neurites, apoptotic neurons, and reduced inflammation in cortical multiple sclerosis lesions. Ann. Neurol. *50*, 389–400.

Planche, V., Panatier, A., Hiba, B., Ducourneau, E.G., Raffard, G., Dubourdieu, N., Maitre, M., Lesté-Lasserre, T., Brochet, B., Dousset, V., et al. (2017). Selective dentate gyrus disruption causes memory impairment at the early stage of experimental multiple sclerosis. Brain Behav. Immun. *60*, 240–254.

Pluchino, S., and Cossetti, C. (2013). How stem cells speak with host immune cells in inflammatory brain diseases. Glia *61*, 1379–1401.

Pluchino, S., Quattrini, A., Brambilla, E., Gritti, A., Salani, G., Dina, G., Galli, R., Del Carro, U., Amadio, S., Bergami, A., et al. (2003). Injection of adult neurospheres induces recovery in a chronic model of multiple sclerosis. Nature *422*, 688–694.

Pluchino, S., Zanotti, L., Rossi, B., Brambilla, E., Ottoboni, L., Salani, G., Martinello, M., Cattalini, A., Bergami, A., Furlan, R., et al. (2005). Neurosphere-derived multipotent precursors promote neuroprotection by an immunomodulatory mechanism. Nature *436*, 266–271.

Pluchino, S., Muzio, L., Imitola, J., Deleidi, M., Alfaro-Cervello, C., Salani, G., Porcheri, C., Brambilla, E., Cavasinni, F., Bergamaschi, A., et al. (2008). Persistent inflammation alters the function of the endogenous brain stem cell compartment. Brain *131*, 2564–2578.

Pluchino, S., Gritti, A., Blezer, E., Amadio, S., Brambilla, E., Borsellino, G., Cossetti, C., Del Carro, U., Comi, G., 't Hart, B., et al. (2009a). Human neural stem cells ameliorate autoimmune encephalomyelitis in non-human primates. Ann. Neurol. *66*, 343–354.

Pluchino, S., Zanotti, L., Brambilla, E., Rovere-Querini, P., Capobianco, A., Alfaro-Cervello, C., Salani, G., Cossetti, C., Borsellino, G., Battistini, L., et al. (2009b). Immune regulatory neural stem/precursor cells protect from central nervous system autoimmunity by restraining dendritic cell function. PLoS ONE *4*, e5959.

Prineas, J.W., Kwon, E.E., Cho, E.S., Sharer, L.R., Barnett, M.H., Oleszak, E.L., Hoffman, B., and Morgan, B.P. (2001). Immunopathology of secondary-progressive multiple sclerosis. Ann. Neurol. *50*, 646–657.

Ramos-Zúñiga, R., González-Pérez, O., Macías-Ornelas, A., Capilla-González, V., and Quiñones-Hinojosa, A. (2012). Ethical implications in the use of embryonic and adult neural stem cells. Stem Cells Int. *2012*, 470949.

Rice, C.M., Kemp, K., Wilkins, A., and Scolding, N.J. (2013). Cell therapy for multiple sclerosis: an evolving concept with implications for other neurodegenerative diseases. Lancet *382*, 1204–1213.

Ritchie, M.E., Phipson, B., Wu, D., Hu, Y., Law, C.W., Shi, W., and Smyth, G.K. (2015). limma powers differential expression analyses for RNA-sequencing and microarray studies. Nucleic Acids Res. *43*, e47.

Rubic, T., Lametschwandtner, G., Jost, S., Hinteregger, S., Kund, J., Carballido-Perrig, N., Schwärzler, C., Junt, T., Voshol, H., Meingassner, J.G., et al. (2008). Triggering the succinate receptor GPR91 on dendritic cells enhances immunity. Nat. Immunol. *9*, 1261–1269.

Ryu, J.K., Nagai, A., Kim, J., Lee, M.C., McLarnon, J.G., and Kim, S.U. (2003). Microglial activation and cell death induced by the mitochondrial toxin 3-nitropropionic acid: in vitro and in vivo studies. Neurobiol. Dis. *12*, 121–132.

Shinawi, M., Gruener, N., and Lerner, A. (1998). CSF levels of carnitine in children with meningitis, neurologic disorders, acute gastroenteritis, and seizure. Neurology *50*, 1869–1871.

Srisawang, P., Chatsudthipong, A., and Chatsudthipong, V. (2007). Modulation of succinate transport in Hep G2 cell line by PKC. Biochim. Biophys. Acta *1768*, 1378–1388.

Tambalo, S., Peruzzotti-Jametti, L., Rigolio, R., Fiorini, S., Bontempi, P., Mallucci, G., Balzarotti, B., Marmiroli, P., Sbarbati, A., Cavaletti, G., et al. (2015). Functional magnetic resonance imaging of rats with experimental autoimmune encephalomyelitis reveals brain cortex remodeling. J. Neurosci. *35*, 10088–10100.

Tannahill, G.M., Curtis, A.M., Adamik, J., Palsson-McDermott, E.M., McGettrick, A.F., Goel, G., Frezza, C., Bernard, N.J., Kelly, B., Foley, N.H., et al. (2013). Succinate is an inflammatory signal that induces IL-1β through HIF-1α. Nature *496*, 238–242.

Tannahill, G.M., Iraci, N., Gaude, E., Frezza, C., and Pluchino, S. (2015). Metabolic reprograming of mononuclear phagocytes in progressive multiple sclerosis. Front. Immunol. *6*, 106.

Thier, M., Wörsdörfer, P., Lakes, Y.B., Gorris, R., Herms, S., Opitz, T., Seiferling, D., Quandel, T., Hoffmann, P., Nöthen, M.M., et al. (2012). Direct conversion of fibroblasts into stably expandable neural stem cells. Cell Stem Cell *10*, 473–479.

Vasandan, A.B., Jahnavi, S., Shashank, C., Prasad, P., Kumar, A., and Prasanna, S.J. (2016). Human Mesenchymal stem cells program macrophage plasticity by altering their metabolic status via a PGE2-dependent mechanism. Sci. Rep. *6*, 38308.

Vescovi, A.L., and Snyder, E.Y. (1999). Establishment and properties of neural stem cell clones: plasticity in vitro and in vivo. Brain Pathol. *9*, 569–598.

Volpe, G., Bernstock, J.D., Peruzzotti-Jametti, L., and Pluchino, S. (2016). Modulation of host immune responses following non-hematopoietic stem cell transplantation: Translational implications in progressive multiple sclerosis. J. Neuroimmunol., S0165-5728(16)30312-5.

Wang, H.L., and Lai, T.W. (2014). Optimization of Evans blue quantitation in limited rat tissue samples. Sci. Rep. *4*, 6588.

Wikoff, W.R., Pendyala, G., Siuzdak, G., and Fox, H.S. (2008). Metabolomic analysis of the cerebrospinal fluid reveals changes in phospholipase expression in the CNS of SIV-infected macaques. J. Clin. Invest. *118*, 2661–2669.

Wörsdörfer, P., Thier, M., Kadari, A., and Edenhofer, F. (2013). Roadmap to cellular reprogramming–manipulating transcriptional networks with DNA, RNA, proteins and small molecules. Curr. Mol. Med. *13*, 868–878.

Wright, L.S., Prowse, K.R., Wallace, K., Linskens, M.H., and Svendsen, C.N. (2006). Human progenitor cells isolated from the developing cortex undergo decreased neurogenesis and eventual senescence following expansion in vitro. Exp. Cell Res. *312*, 2107–2120.

Yañez, R., Oviedo, A., Aldea, M., Bueren, J.A., and Lamana, M.L. (2010). Prostaglandin E2 plays a key role in the immunosuppressive properties of adipose and bone marrow tissue-derived mesenchymal stromal cells. Exp. Cell Res. *316*, 3109–3123.